1 **Visualization and regulation of translocons in *Yersinia* type III protein**

2 **secretion machines during host cell infection**

3

4 Theresa Nauth[1][¶], Franziska Huschka[1][¶], Michaela Schweizer[2], Jens B. Bosse[3], Andreas

5 Diepold[4], Antonio V. Failla[5], Anika Steffen[6], Theresia Stradal[6], Manuel Wolters[1][&], Martin

6 Aepfelbacher[1][&][*]

7

8 [1] Institute of Medical Microbiology, Virology and Hygiene and [2] Center for Molecular

9 Neurobiology (ZMNH), University Medical Center Hamburg-Eppendorf (UKE), Hamburg,

10 Germany; [3] Heinrich Pette Institute, Leibniz Institute for Experimental Virology (HPI),

11 Hamburg, Germany; [4] Department of Ecophysiology, Max Planck Institute for Terrestial

12 Microbiology, Marburg, Germany; [5] UKE Microscopy Imaging Facility, University Medical

13 Center Hamburg-Eppendorf (UKE), Hamburg, Germany; [6] Department of Cell Biology,

14 Helmholtz Centre for Infection Research (HZI), Braunschweig, Germany.

15

16 *corresponding author; E-mail: m.aepfelbacher@uke.de

17

18 [¶][&]These two groups of authors contributed equally to this work. The authors have

19 declared that no competing interests exist.

20

21 Conceived and designed experiments: TN FH MW MA; Performed experiments: TN FH

22 MW MS; Analyzed the data: TN FH MW JB; Contributed reagents/materials/analysis

23 tools/microscopes: MS AS VF TS JB AD; Wrote the paper: MA TN MW.

24

25 Abstract

26   Type III secretion systems (T3SSs) are essential virulence factors of numerous bacterial

27   pathogens. Upon host cell contact the T3SS machinery - also named injectisome -

28   assembles a pore complex/translocon within host cell membranes that serves as an

29   entry gate for the bacterial effectors. Whether and how translocons are physically

30   connected to injectisome needles, whether their phenotype is related to the level of

31   effector translocation and which target cell factors trigger their assembly have remained

32   unclear. We employed the superresolution fluorescence microscopy techniques

33   Stimulated Emission Depletion (STED) and Structured Illumination Microscopy (SIM) as

34   well as immunogold electron microscopy to visualize *Y. enterocolitica* translocons

35   during infection of different target cell types. Thereby we were able to resolve

36   translocon and needle complex proteins within the same injectisomes and demonstrate

37   that these fully assembled injectisomes are generated in a prevacuole, a PI(4,5)P2

38   enriched host cell compartment inaccessible to large extracellular proteins like

39   antibodies. Furthermore, the putatively operable translocons were produced by the

40   yersiniae to a much larger degree in macrophages (up to 25% of bacteria) than in HeLa

41   cells (2% of bacteria). However, when the Rho GTPase Rac1 was activated in the HeLa

42   cells, uptake of the yersiniae into the prevacuole, translocon formation and effector

43   translocation were strongly enhanced reaching the same levels as in macrophages. Our

44   findings indicate that operable T3SS translocons can be visualized as part of fully

45   assembled injectisomes with superresolution fluorescence microscopy techniques. By

46   using this technology we provide novel information about the spatiotemporal

47   organisation of T3SS translocons and their regulation by host cell factors.

48

Author Summary

Many human, animal and plant pathogenic bacteria employ a molecular machine termed injectisome to inject their toxins into host cells. Because injectisomes are crucial for these bacteria's infectious potential they have been considered as targets for antiinfective drugs. Injectisomes are highly similar between the different bacterial pathogens and most of their overall structure is well established at the molecular level. However, only little information is available for a central part of the injectisome named the translocon. This pore-like assembly integrates into host cell membranes and thereby serves as an entry gate for the bacterial toxins. We used state of the art fluorescence microscopy to watch translocons of the diarrheagenic pathogen *Yersinia enterocolitica* during infection of human host cells. Thereby we could for the first time - with fluorescence microscopy - visualize translocons connected to other parts of the injectisome. Furthermore, because translocons mark functional injectisomes we could obtain evidence that injectisomes only become active when the bacteria are almost completely enclosed by host cells. These findings provide a novel view on the organisation and regulation of bacterial translocons and may thus open up new strategies to block the function of infectious bacteria.

Introduction

Bacterial type III secretion systems (T3SSs) are molecular machines also termed injectisomes that translocate proteins of bacterial origin (i.e. effectors) into host cells. T3SSs are essential virulence factors of numerous human, animal and plant pathogens including *Chlamydia*, *Pseudomonas*, EPEC and EHEC, *Salmonella*, *Shigella* and *Yersinia* [2, 3]. Based on sequence identity among structural components nine T3SS families were classified [4]. Whereas assembly, structure and function of the T3SSs are highly conserved, the biochemical activities of the translocated effectors often are multifaceted and reflect the infection strategies of the individual pathogens [5]. Because of their uniqueness in bacteria on one hand and central role for bacterial pathogenicity on the other hand T3SSs have been considered as targets for novel antiinfective strategies [6–9]. In addition, the ability of T3SSs to inject arbitrary proteins into immune cells has been exploited for experimental vaccination strategies [10].

Based on topology and function injectisomes can be separated into different parts: i) the sorting platform on the cytoplasmic side of the injectisome is a protein assembly thought to control targeting and secretion of the T3SS substrates; ii) the basal body including the export apparatus spans the inner and outer bacterial membranes; iii) the 30-70 nm long needle filament is built by a single multimerized protein and together with the basal body forms the needle complex; iv) the tip complex consists of a hydrophilic protein that caps the needle filament and regulates assembly of the translocon; v) the translocon consists of two hydrophobic translocator proteins that upon host cell contact form a pore in the host cell membrane serving as a regulated entry gate for the bacterial effectors (Figure 3A) [1–3, 8, 11–15].

Assembly of the injectisome starts with formation of the basal body by the bacterial Sec system and is followed by export of the needle proteins as early T3SS substrates. The

4

91   tube-like needle then allows passage of the tip complex and translocon proteins, which

92   are intermediate substrates. Bacterial effector proteins, representing the late T3SS

93   substrates, are thought to be translocated into host cells through a conduit formed by

94   needle complex and translocon.

95   Although electron microscopy, crystallography and biophysical techniques have

96   provided a high resolution picture of the assembly and architecture of needle complex

97   and sorting platform [6], major properties of the translocon such as its composition,

98   exact localization - i.e. attached to or separated from the needle tip - or regulation have

99   remained elusive or controversial [16].

100   All investigated T3SSs express two hydrophobic translocators, a major translocator

101   harboring two and a minor translocator harboring one transmembrane domain [14, 17].

102   Numerous studies suggested that both translocators are required for a functional

103   translocon and assemble into a heteromultimeric pore complex [14, 17]. Although T3SS

104   translocation pores have not been visualized directly in situ, the inner opening of the

105   pore is thought to have a diameter of 2-4 nm, as estimated by in vitro reconstitution,

106   osmoprotection and dextran release assays [17–24]. Reconstitution in liposomes

107   suggested that the *P. aeruginosa* translocators PopB and PopD, which are highly

108   homologous to *Yersinia* YopB and YopD, form a hexadecameric 8:8 complex [25]. A pore

109   complex transferred by *Y. enterocolitica* into erythrocyte membranes displayed a

110   molecular weight of 500-700 kD [26]. Of note, considering the approximate molecular

111   weights of 44 kD for YopB and 34 kD for YopD, a 8:8 complex of YopB and YopD would

112   have an expected molecular weight of around 624 kD.

113   A previous report challenged the paradigm that effector translocation by *Yersinia*

114   *pseudotuberculosis* proceeds through a continuous conduit from the bacterium directly

115   into the target cell. Rather, it was proposed that isolated effectors located on the surface

116   of the bacteria can translocate into target cells with the help of a separate and even an

117   unrelated *Salmonella* T3SS [16].

118   It has become clear that effector translocation as well as isolated pore activities of

119   T3SSs, such as disruption of cells and increased permeability of cell membranes, are

120   regulated by diverse host factors including actin, Rho proteins, cholesterol,

121   sphingolipids, coatomers, clathrin and exocyst [27–30]. In *Yersinia*, filamentous (f)-actin

122   disruption and Rho GTPase inhibitors block translocation of effector Yops and YopB/D

123   pore activity, whereas activation of Rho GTPases enhances effector Yop translocation

124   [31–35]. In addition, in a feedback mechanism pathogenic yersiniae can control T3SS

125   function through their own effectors, i.e. by modulating Rho protein activity in host cells

126   [27].

127   In this work we performed high resolution fluorescence and immunogold electron

128   microscopy to visualize translocons of *Y. enterocolitica* during host cell infection.

129   Thereby we deciphered that translocons are connected to the remaining T3SS, that their

130   overall number is changed dependent on the level of effector translocation and that they

131   are formed in a specific host cell compartment.

132

133   **Results**

134   ***Yersinia* translocators YopB and YopD localize on the bacterial cell surface after**

135   **secretion by the T3SS**

136   During infection with pathogenic yersiniae the translocators YopB and YopD are

137   inserted into host cell membranes where they form a pore (also termed translocon) that

138   acts as an entry gate for the *Yersinia* effectors [18, 21, 26]. To visualize the *Yersinia*

139   translocators YopB and YopD we produced specific rabbit and rat polyclonal antibodies

140   (S1 Fig A and B for antibody specificity). In lysates of *Y. enterocolitica* WA-314 (wild

141   type; table 1) grown at 27°C, YopB and YopD could not be detected by immunoblot.

142   Table 1. Yersinia strains

Strain	Relevant characteristic	Source/References
Yersinia enterocolitica		
WA-314	Wild-type strain carrying virulence plasmid pYV; serogroup O8; kanamycin resistance cassette in non-coding region of pYV-O8	[40, 41]
WA-C	pYV-cured derivative of WA-314	[40]
WA-314ΔYopE	WA-C harboring pYVΔYopE; Kan^R	[42]
WA-314ΔYopD	WA-C harboring pYVΔYopD; Kan^R	this work
WA-314ΔYopB	WA-C harboring pYVΔYopB; Kan^R	this work
E40 GFP-YscD	E40 pAD4306; serogroup O9; pYVe40 ($yopO_{\Delta2-427}$ $yopE_{21}$ $yopH_{\Delta1-352}$ $yopM_{23}$ $yopP_{23}$ $yopT_{135}$ $egfp$-$yscD$); $asd_{\Delta292-610}$ (auxotrophic for diaminopimelic acid)	[1]

143

144   However, YopB and YopD proteins became detectable in bacteria grown at 37°C in high

145   Ca^{2+} medium (non-secretion condition) and their levels further increased in bacteria

146   grown in low Ca^{2+} medium (secretion condition; Fig 1A). It is well accepted that *Yersinia*

147   T3SS gene expression is switched on at 37°C and that depletion of Ca^{2+} from the *Yersinia*

148   growth medium triggers Yop secretion and boosts Yop production in a process named

149   low Ca^{2+} response [36–38]. YopB and YopD were immunofluorescence-stained in

150   *Yersinia* wild type at secretion condition using a procedure not supposed to

151   permeabilize the bacterial double membrane. By confocal microscopy intense YopB and

152   YopD fluorescence signals were seen along the bacterial circumference in essentially

153   100% of the bacteria (Fig 1B, C and S1 Fig C). In comparison, essentially no YopB/YopD

154   immunofluorescence signals were found in bacteria at non-secretion condition and in

7

155 bacteria at secretion condition which were treated with proteinase K (PK) before

156 staining (Fig 1B and S1 Fig C upper panel and 1C). When immunostaining was

157 performed in the presence of 2% sodium dodecyl sulfate (SDS) to permeabilize the

158 bacterial double membrane, essentially all bacteria at non-secretion and secretion

159 conditions displayed YopB and YopD signals (Fig 1B and C; S1 Fig C). In this case the

160 YopB/YopD signals filled the whole bacterial cell rather than just the cell periphery,

161 indicating that also intrabacterial pools of the proteins were stained. Accordingly,

162 addition of proteinase K before staining of the bacteria under permeabilizing condition

163 did not alter the YopB signal (Fig 1B and S1 Fig C). Total YopB signals were considerably

164 higher in bacteria at secretion than at non-secretion condition, consistent with the

165 immunoblot data (Fig 1A and B; S1 Fig A and C).

166 To visualize YopB and YopD on the bacterial surface with higher spatial resolution, we

167 employed stimulated emission depletion (STED) microscopy [39]. STED microscopy

168 increases resolution of fluorescence signals to approximately 30-80 nm under the

169 condition used (lateral resolution at 100% 2-D STED). The YopB and YopD fluorescence

170 signals recorded with STED microscopy appeared sharper and confined to a narrow

171 band encompassing the bacterial periphery when compared to the signals obtained with

172 confocal microscopy (Fig 1D). Co-immunostaining revealed no systematic colocalization

173 of YopB and YopD on the bacterial surface as demonstrated by merge of YopB and YopD

174 3D-STED images and by superimposed intensity plots of the YopB and YopD signals on

175 the bacterial surface (Fig 1D).

176 We conclude that during the low Ca^{2+}-response the secreted translocators YopB and

177 YopD localize on the *Yersinia* cell surface but do not display a specific (co)localization

178 pattern when investigated with high resolution fluorescence microscopy.

179

8

180   YopB and YopD associate with injectisomes during cell infection

181   In order to visualize operational translocons, YopB and YopD were immunostained

182   during *Y. enterocolitica* infection of HeLa cells and primary human macrophages.

183   Confocal micrographs revealed that YopB and YopD concentrate in distinct patches in

184   host cell associated wild type bacteria (Fig 2A and S2 Fig A). This clustered appearance

185   as imaged by confocal microscopy was in clear contrast to the more uniform YopB/YopD

186   distribution in secreting bacteria (Fig 1B and D). Time course experiments

187   demonstrated that the fraction of wild type bacteria that stained positive for YopB in

188   HeLa cells reached only about 2% at 60 min post infection (Fig 2B). By comparison, in

189   human macrophages, which represent more physiological target cells of pathogenic

190   yersiniae [33, 43, 44], the fraction of YopB positive bacteria amounted to around 25% at

191   20 min post infection (Fig 2B).

192   We next investigated the YopB signals in HeLa cells using confocal and STED microscopy

193   in parallel. In strain WA-314ΔYopE (table1), which was well suited for this analysis

194   because it displayed a much higher percentage of YopB positive bacteria than wild type

195   (see below), single patches in the confocal recordings could regularly be resolved into 3

196   distinct spots with the STED technology (Fig 2C). In the mean around 11 YopB positive

197   patches and 33 YopB positive spots were detected per bacterium when investigated

198   with confocal- and STED microscopy, respectively (Fig 2C). For a more comprehensive

199   evaluation of the organisation of the YopB spots on the bacterial surface they were

200   recorded in 3D-STED mode and subjected to image analysis. Spot detection and

201   segmentation as well as cluster analysis revealed that the YopB spots are regularly

202   organized in clusters with on average 2.8 ± 1 spots per cluster. The mean distance

203   between the spots in one cluster was 127 ± 42 nm and the mean distance between

204   individual clusters was 713 ± 121 nm (mean ± S.D., n=64; Methods). To exemplarily

205   visualize the distribution of all identified clusters on a single bacterial cell,

206   superresolution 3D images were prepared in which each segmented cluster is

207   represented by a different color and the bacterium is viewed from different angles (Fig.

208   2C' and S2 Fig B and S1 movie; Methods).

209   We reasoned that if the YopB and YopD spots detected by STED microscopy reflect

210   translocons associated with the injectisome, YopB and YopD should colocalize with each

211   other as well as with the tip complex protein LcrV, which is essential for linking

212   YopB/YopD to the needle tip [45, 46]. YopB and YopD showed a complete colocalization

213   in host cell associated bacteria, which was best documented when colocalizing points or

214   intensity plots of YopB and YopD fluorescence on the bacterial surface were determined

215   (Fig 2D and 2D'). Furthermore, STED images of YopB and LcrV co-immunostaining

216   indicated that essentially all YopB signals are associated with LcrV signals (Fig 2D). The

217   LcrV staining was less bright than the YopB staining which may result from the lower

218   number of LcrV molecules per injectisome [47–49].

219   To further support the notion that the YopB/YopD fluorescence signals in the cell

220   associated bacteria represent translocons attached to needle tips, we investigated the

221   spatial coupling of YopB/D to the basal body component YscD at high resolution.

222   Considering the published data on *Yersinia* basal body, needle and tip complex length as

223   well recent work in *Salmonella*, the N-terminal domain of YscD - or of its homologues - is

224   located in approximately 100 nm distance from the needle tip (Fig 3A, [13, 50–53]). For

225   this experiment HeLa cells were infected with *Y. enterocolitica* strain E40 GFP-YscD [1]

226   (table1) expressing a N-terminal EGFP-fusion of YscD and immunostained for YopB or

227   YopD. Because GFP-YscD did not produce a high enough fluorescence signal for STED

228   microscopy, the alternative high resolution microscopy technique structured

229   illumination microscopy (3D-SIM, resolution to ~100 nm in x-y plane, [54, 55]) was

10

230   employed to visualize GFP-YscD and YopB/D in parallel. SIM revealed single YopB dots

231   that could clearly be separated from each other and from neighboring patches of GFP-

232   YscD (Fig 3B). A fluorescence intensity plot of a representative YopB/GFP-YscD pair

233   indicated a distance of 90 nm between the fluorescence maxima (Fig 3B). A more

234   comprehensive nearest neighbour analysis indicated distances between the GFP-YscD

235   patches and YopB/D dots of around 110 nm (109 ±4 nm; n=424 pairs evaluated;

236   Methods; Fig 3C).

237   Having successfully resolved fluorescence signals from translocon and basal body

238   proteins that are located in distant parts of the same injectisomes, we next

239   coimmunostained the needle protein YscF with YopB in strain E40 GFP-YscD. YscF forms

240   the needle that connects translocon and basal body in injectisomes (Fig 3A). SIM

241   revealed tripartite complexes made up of YopB, GFP-YscD and YscF, whereby the

242   fluorescence signal for YscF was sandwiched between the YopB and YscD signals (Fig

243   3D). Thus, by high resolution SIM we were able to resolve three proteins located in

244   different parts of *Yersinia* injectisomes.

245   We next aimed to visualize YopD and GFP-YscD embedded in their native bacterial and

246   host cellular environment. Transmission electron microscopy (TEM) of ultrathin

247   sections combined with cryoimmunolabelling allows high resolution localization of

248   proteins within their cellular context [56, 57]. Electron-dense protein-A/gold particles

249   of different sizes (usually 5-15 nm) additionally permit to localize different proteins in

250   the same sections [58]. We infected Rac1Q61L expressing HeLa cells, in which the

251   expression of *Yersinia* injectisomes is strongly enhanced (see below), with strain E40

252   GFP-YscD and immunolabelled YopD and GFP-YscD with 10 nm and 15 nm gold

253   particles, respectively. The labelling density of the 10 nm gold particles marking YopD

254   was much higher in the bacterial cell (cytoplasm and double membrane; relative

11

255   labelling index (RLI: 2.73) than in the extrabacterial area (RLI: 0.42; Fig 3E and S1 table

256   A). Thus, the observed distribution of the 10 nm gold particles reflects the expected

257   YopD localization in section staining, which includes the injectisome and the

258   intrabacterial pools (S1 Fig C). We next aimed to assess if the extrabacterially located 10

259   nm gold particles could represent YopD in translocons at the tip of injectisome needles.

260   We assumed that in this case the gold particles should be located within a range of 90

261   nm from the bacterial outer membrane which we defined as injectisome range,

262   reflecting the cumulative dimensions of the injectisome needle (~60 nm), tip complex

263   (~8 nm) and antibody/protein A complex used for immunogold staining (~20 nm; Fig

264   3E). Distances less than 90 nm may occur depending on the geometry and spatial

265   orientation of the type III secretion machines in the 2D analysis.

266   YopD labelling within the injectisome range was significantly enriched (RLI: 2.16)

267   compared to the remaining host cell area (RLI: 0.79; Fig 3E and S1 table B) suggesting

268   that it represents translocons associated with injectisomes.

269   The labelling density of the gold particles marking GFP-YscD was highest in the bacterial

270   double membrane (RLI: 4.44) followed by the bacterial cytoplasm (RLI: 2.38) and was

271   only minor in the extrabacterial space (RLI: 0.52; Fig 3E and S1 table C). This

272   distribution reflects the expected localization of GFP-YscD in assembled basal bodies in

273   the inner bacterial membrane and in an intrabacterial YscD pool. We finally employed

274   co-immunogold staining to detect GFP-YscD and YopD localized within the same

275   injectisomes. Considering the dimensions of the injectisome (length of ~100 nm; Fig 3A)

276   and the two antibody/protein A complexes (length of 2 x 20 nm = 40 nm), we assumed

277   that 10 nm gold particles (YopD label) that lie extrabacterially and in an at most ~140

278   nm distance from 15 nm gold particles, that themselves are located in the bacterial

279   double membrane (YscD label), belong to the same fully assembled injectisome.

12

280   Consistent with this notion we repeatedly identified configurations of 10 nm and 15 nm

281   gold particles fulfilling these premises (Fig 3E'). Of note, the 10 nm gold particles were

282   often found in close proximity to the host cell membrane surrounding the bacteria (Fig

283   3E'). Thus, the observed distributions of the 10 nm and 15 nm gold particles in bacteria

284   surrounded by host cell membranes reflect the expected locations of YopD and GFP-

285   YscD at the tip and basal body, respectively, of injectisomes.

286   In summary, we conclude that the *Yersinia* translocons can be visualized in fully

287   assembled injectisomes by superresolution fluorescence microscopy (SIM and STED)

288   and immunogold TEM techniques, the latter method also suggesting that translocons are

289   located in a specific cellular compartment.

290

291   **Rac1 activity and host cell type regulate *Yersinia* translocon formation**

292   The visualization of putatively operable translocons in host cells prompted us to test

293   how translocon number or distribution correlate with the level of effector translocation.

294   To enhance Yop effector translocation into HeLa cells, cells were infected with the YopE-

295   deficient strain WA-314ΔYopE or cells expressing the constitutively active Rho GTP-

296   binding protein Rac1Q61L were infected with wild type *Yersinia*. Under these conditions

297   Yop-translocation rates increase 5-10-fold [35] which is a consequence of the elevated

298   Rac activity in the host cells [35, 59, 60]. In the case of WA-314ΔYopE the elevated Rac

299   activity is caused by the diminished Rac inhibition that is normally imposed by the Rho

300   GTPase-activatingprotein YopE [61, 62]. Notably, the fraction of YopB positive bacteria

301   increased from around 2% in wild type infected cells to 30% in WA-314ΔYopE infected

302   cells and also reached around 30% in the Rac1Q61L expressing and wild type infected

303   cells at 1 h post infection (Fig 4A).

13

304   As an alternative method to detect host membrane inserted translocons we employed a

305   digitonin-based release assay. Digitonin extracts host cell associated Yops but not

306   intrabacterial Yops and has hitherto been used to assay effector-Yop translocation [63].

307   Consistent with an increased deposition of translocons in the infected cells, the amounts

308   of YopB and YopD extracted by digitonin were increased in the WA-314ΔYopE infected

309   cells as well as in the wild type infected and Rac1Q61L expressing cells when compared

310   to the respective controls (Fig 4B). The extracted amounts of YopB and YopD correlated

311   with the extracted amount of YopH, the latter serving as a measure for effector-Yop

312   translocation (Fig 4B). In comparison, the levels of YopB, YopD and HSP60 in the pellet

313   fraction (representing the bacterial protein pool) were similar in all conditions.

314   Thus, in infected HeLa cells stimulation of Yop translocation is associated with a large

315   increase in the number of bacteria forming translocons which causes enhanced

316   translocon incorporation into cell membranes.

317   We next tested whether the number of translocons per bacterium, as identified by YopB

318   fluorescence spots in STED images, was also altered under conditions of increased Yop

319   translocation. In strain WA-314ΔYopE the number of translocons was nearly twice as

320   high as that in wild type upon infection of HeLa cells (Fig 4C). Furthermore, in

321   macrophages wild type bacteria showed a significantly higher number of translocons

322   than in HeLa cells reaching similar values as WA-314ΔYopE in HeLa cells (Fig 4C). There

323   was no difference in the number of translocons formed between wild type and WA-

324   314ΔYopE in macrophages (Fig 4C) excluding that the WA-314ΔYopE strain intrinsically

325   produces more translocons. Interestingly, in macrophages there was also no difference

326   in the fraction of translocon positive bacteria between wild type and WA-314ΔYopE (Fig

327   4D).

328　These results indicate that host factors not only regulate the number of bacteria

329　producing translocons and thereby the level of translocons within cell membranes but

330　also can affect the number of translocons/injectisomes per bacterium. They also indicate

331　that macrophages can trigger pathogenic yersiniae much more effectively than HeLa

332　cells to produce translocons. Of note, upon activation of Rac HeLa cells acquire the same

333　potency as macrophages in stimulating translocon formation whereas translocon

334　formation in the already highly effective macrophages appears not to be affected (Fig 2B

335　and 4D).

336

337　**Formation of translocons is triggered in a prevacuole, a PI(4,5)P2 enriched host**

338　**cell compartment**

339　The TEM images showed translocons in yersiniae enclosed by host cell membranes. This

340　prompted us to test whether formation of translocons is triggered in a specific host cell

341　compartment. Previously it was described that during cell invasion avirulent yersiniae

342　enter a precompartment in which they are accessible to externally administered small

343　proteins or compounds (MW 50 kD) but not to antibodies (MW around 150 kD, [64,

344　65]). This compartment was named a prevacuole and shown to be enriched in the

345　phospholipid PI(4,5)P2 [64].

346　When Hela cells were infected with biotinylated wild type *Y. enterocolitica* for 60 min

347　and bacterial accessibility to externally administered streptavidin (MW 53 kD) or

348　*Yersinia* specific antibodies was assessed by fluorescence staining, three different

349　staining patterns were found. The bacteria were either accessible to antibodies and

350　streptavidin (denominated outside), inaccessible to antibodies but accessible to

351　streptavidin (intermediary) or inaccessible to both, antibodies and streptavidin (inside;

352　Fig 5A and 5A'). Quantitative analysis showed that about 70% of the YopB positive

15

353   bacteria were located in the intermediary compartment and around 25% in the inside

354   compartment but only a negligible fraction (less than 5%) was present in the outside

355   localization at 1 h post infection (Fig 5A").

356   To find out in which macrophage compartment translocons are formed, we assayed

357   YopB fluorescence signals of bacteria during their passage into the intermediary and

358   inside compartments. For this macrophages prepared from four different donors were

359   infected with wild type and investigated during a 60 min time period. The bacteria

360   started to enter the intermediary compartment before 5 min of infection (Fig 5B) and in

361   all but one preparation of macrophages (donor 4, Fig 5B) the fraction of bacteria that

362   localized to the intermediary compartment remained stable between 20 to 60 min post

363   infection. At 60 min post infection 20 to 40% of the cell associated bacteria still resided

364   in the intermediary compartments (Fig 5B). Notably, the fraction of bacteria that further

365   progressed to the inside compartment differed widely among the different macrophage

366   preparations. It amounted to 60-80% in macrophages from donors 1 and 2 and was

367   about 5% in macrophages from donors 3 and 4 at 60min post infection (Fig 5B). Thus in

368   macrophages from some individuals only a minimal fraction of wild type *Yersinia*

369   transits from the intermediary to the inside compartment, whereas in macrophages

370   from other donors the bacteria readily proceed to the inside compartment.

371   In a preparation of macrophages in which the bacteria mostly end up in the inside

372   compartment (similar to macrophages from donor 1, Fig 5B) it was first verified that

373   bacteria in the outside location do not show YopB staining like already seen in HeLa cells

374   (no YopB positive outside bacteria in 50 macrophages from two experiments

375   investigated). At 5-10 min post infection essentially all YopB positive bacteria were

376   found in the intermediary compartment and thereafter the fraction of YopB positive

377   bacteria decreased in the intermediary compartment and in parallel increased in the

16

378   inside compartment (Fig 5C). These results clearly indicate that translocons are formed

379   in the intermediary compartment of macrophages and then are carried on to the inside

380   compartment.

381   That the translocon proteins in the intermediary compartment are accessible to

382   externally added proteins was confirmed with a modified digitonin lysis assay.

383   Proteinase K (MW 29 kD) was added to *Yersinia* WA-314 or WA-314ΔYopE infected

384   HeLa cells and was then neutralized with phenylmethylsulfonyl fluoride (PMSF) prior to

385   digitonin lysis and Western blot analysis of the cells. Under these conditions YopB and

386   YopD were largely degraded whereas the effector YopH and actin remained unchanged

387   (Fig 5F). It was verified in control experiments that with the proteinase K amounts

388   employed Yops can principally be degraded and that addition of PMSF abrogates

389   proteinase K activity (S3 Fig A, Methods).

390   The prevacuole formed during invasion of avirulent *Y. pseudotuberculosis* into COS1 cells

391   was characterized by accumulation of the PI(4,5)P2 sensor PLCδ-PH-GFP [64].

392   Accumulation of PLCδ-PH-GFP also marked the intermediary compartment in wild type

393   infected HeLa cells (Fig 5D) and accumulated around translocon positive wild type

394   bacteria in human macrophages (Fig 5E).

395   We finally hypothesized that the strong enhancement of translocon formation in HeLa

396   cells upon Rac1 activation may be due to the capability of Rac to stimulate bacterial

397   uptake into the intermediary prevacuolar compartment [66–68].

398   In fact, in HeLa cells overexpressing myc-Rac1Q61L around 60% of wild type bacteria

399   became inaccessible to antibodies compared to around 10% in control cells after 1 h of

400   infection (Fig 5G). This resulted in a 6-fold higher number of YopB positive bacteria

401   both, in the intermediary and inside compartments of myc-Rac1Q61L overexpressing

402   cells when compared to controls (Fig 5H).

403   Altogether we conclude from this set of experiments that the formation of *Yersinia*

404   translocons is triggered in a PI(4,5)P2 enriched permissive cell compartment, which is

405   protected from large extracellular proteins like antibodies. Primary human

406   macrophages readily internalise the bacteria in this permissive compartment, which is

407   most certainly the reason why they so effectively stimulate translocon formation. In

408   comparison, epithelial cells like HeLa cells possess a low intrinsic activity to internalise

409   the bacteria in the permissive compartment. However, uptake of the bacteria into the

410   permissive compartment, translocon formation and effector translocation can be

411   dramatically stimulated to values reached in primary macrophages by activation of the

412   Rho GTP binding protein Rac1.

413

414   **Discussion**

415   The two hydrophobic translocators present in most T3SSs and the pore

416   complex/translocon that these proteins form in host cell membranes are particularly

417   difficult to investigate. This is amongst others due to the highly elaborate transit of the

418   translocators from the bacterial interior where they have to be in a soluble form,

419   through the T3SS needle when they are in an unfolded state, up to their dynamic

420   interaction with the needle tip. The tip complex is supposed to orchestrate integration of

421   the translocators into the host cell membrane, a process that presumably is

422   accompanied by refolding and heteromultimeric assembly of the proteins. Because it is

423   localized at the interface of the bacterial T3SS and the target cell membrane, the

424   translocon is unavoidably controlled by host cell factors that determine the composition

425   and function of cell membranes.

426   A recent superresolution fluorescence microscopy study of *Salmonella* Typhimurium

427   without host cell contact described clusters of the basal body protein PrgH, a *Yersinia*

18

428 YscD analogon, with a width of 46 nm [50]. The 12 PrgH clusters found on average per

429 *Salmonella* cell were shown to represent individual needle complexes whereby the mean

430 distance between the PrgH fluorescent signal and the signal of the tip complex protein

431 SipD, a *Yersinia* LcrV analogon, was determined to be 101 nm [50].

432 Cryo-Electron Tomography (Cryo-ET) analysis of *Y. enterocolitica* (mini)cells also

433 provided an estimation of the number and organization of needle complexes expressed

434 without host cell contact. In tomograms of single *Y. enterocolitica* cells 6.2 injectisomes

435 were detected on average whereby it was calculated that the employed technique

436 underestimates the total number of injectisomes by a factor of 2-3. Cryo-ET also

437 demonstrated that separate fluorescence signals of *Yersinia* needle complexes seen in

438 the confocal microscope contained in the mean 2.5 injectisomes organized in clusters.

439 Within these clusters the injectisomes were about 100 nm apart whereas more

440 randomly distributed injectisomes showed distances of about 400 nm [13]. These

441 numbers are in good agreement with the 18-33 translocons implying fully assembled

442 injectisomes identified by superresolution fluorescence microscopy in *Y. enterocolitica*.

443 They also comply well with the average distance of 127 nm between individual

444 translocons in clusters as well as with the mean distance of 716 nm measured between

445 the clusters. Our data further suggest that the number of operable translocons on the

446 bacteria increases in parallel to effector translocation and is significantly higher in

447 macrophages than in epithelial cells. In fluorescence patches of translocator proteins

448 visualized with confocal microscopy we were able to resolve on average 3 separate

449 translocator spots by STED, corresponding well to the 2-3 injectisomes found with Cryo-

450 ET in fluorescence clusters of injectisome components [13]. The previously reported

451 numbers of injectisomes in secreting bacterial cells, their dimensions and distances

452   among each other is therefore highly concordant with the respective features of the

453   *Yersinia* translocons described here.

454   Until recently a direct view of fully assembled injectisomes including translocons has

455   not been reported. A preprint of a Cryo-ET study provided a first direct view of the T3SS

456   translocon of *Salmonella* minicells during host cell infection [69]. The EM pictures

457   clearly indicate that the *Salmonella* translocon is connected to the T3SS needle and is in

458   parallel embedded in the host cell membrane and protrudes towards the host cell

459   cytoplasm. The *Salmonella* translocons are ~13.5 nm in diameter and 8 nm thick

460   whereby the part of the translocon protruding into the target cell creates a hole which

461   may represent the inner opening through which the effectors enter the cell [69].

462   In this study we employed high resolution STED and SIM fluorescence microscopy to

463   resolve translocon, needle and basal body proteins of *Yersinia* injectisomes during cell

464   infection and come to the conclusion that *Yersinia* injectisomes also form a continuous

465   conduit from the bacterial to the target cell cytoplasm. However, our findings do not

466   exclude the additional existence of translocons operating independently of the

467   remaining injectisome as was proposed recently [16]. Although our high resolution

468   fluorescence data combined with double immunogold staining cannot provide high

469   fidelity structural information like the Cryo-ET technique, fluorescence techniques are

470   accessible to a larger number of researchers and form the basis for future live imaging

471   studies. Moreover, our experiments were not limited to minicells, which do not

472   translocate effectors, and we therefore could identify the role of *Yersinia* effector YopE

473   in regulating translocon formation. Similarly, because we were not restricted to

474   investigation of thin peripheral host cell areas as with Cryo ET, we could characterize a

475   dynamic host cellular compartment that promotes translocon formation. Our study

476   thereby provides an explanation for the reported stimulatory effect of Rho GTP-binding

477   proteins on effector translocation by *Yersinia* [34, 35, 59–62]. We propose that Rac1

478   enhances uptake of yersiniae into the prevacuole of host cells which stimulates

479   formation of operable injectisomes and effector translocation.

480

481

482

483

484

485   **Material and Methods**

486

487   **Materials**

488   All standard laboratory chemicals and supplies were purchased from Roth (Karlsruhe,

489   Germany), Sigma-Aldrich (Steinheim, Germany) or Merck (Hohenbrunn, Germany)

490   unless indicated otherwise.

491

492   **Plasmids**

493   The following plasmids were described previously: PLCδ1-PH-GFP was provided by T.

494   Balla (National Institutes of Health, Bethesda, MD). The myc-Rac1Q61L plasmid was

495   kindly provided by Dr. Pontus Aspenström (Uppsala University, Uppsala, Sweden) and

496   pRK5myc was purchased from Clontech.

497

498   **Antibodies**

499   Polyclonal rabbit anti-YopB (aa 1-168) and anti-YopD (aa 150-287) as well as rat anti-

500   YopB (aa1-168) and anti-YscF antibodies were produced by immunization of the

501   animals with the respective purified GST-fused proteins (animal research project A10a

21

502   675). For immunofluorescence staining, sera were affinity purified by binding either to

503   the suitable GST-fused recombinant antigens bound to glutathione beads or to antigens

504   released by *Y. enterocolitica* WA-314 that were run on SDS-polyacrylamide gel

505   electrophoresis (PAGE) and blotted onto polyvinylidine fluoride (PVDF) membranes

506   (Immobilon-P, Millipore, Schwalbach, Germany). Anti-LcrV, anti-YopH and anti-PepC

507   [70] rabbit polyclonal sera were a gift of Jürgen Heesemann (Max von Pettenkofer-

508   Institute, Munich, Germany).

509   Primary antibodies and their sources were: rabbit polyclonal anti-*Y. enterocolitica* O:8

510   (Sifin, Berlin, Germany); rabbit polyclonal anti-calnexin (Enzo, Lörrach, Germany);

511   rabbit polyclonal myc (Cell Signaling, Cambridge, UK); mouse monoclonal anti-actin

512   (Millipore, Schwalbach, Germany); mouse monoclonal anti-HSP60 and anti-streptavidin-

513   Cy5 (Thermo Fisher Scientific, Waltham, USA); biotin conjugated goat polyclonal anti-

514   GFP (Rockland, Limerick, USA).

515   Secondary anti-IgG antibodies and their sources were: Alexa488 chicken anti-rabbit and

516   goat anti-rat, Alexa568 goat anti-rabbit and goat anti-rat, Alexa647 goat anti-rabbit,

517   Alexa594 chicken anti-rat (Molecular Probes, Karlsruhe, Germany). AbberiorStar580

518   donkey anti-rabbit, AbberiorStarRed donkey anti-rabbit and goat anti-rat,

519   AbberiorStar635P goat anti-rabbit (Abberior, Göttingen, Germany). Rabbit polyclonal

520   anti-biotin (Rockland, Limerick, USA). Protein A gold was purchased from G. Posthuma

521   (University Medical Center Utrecht, Netherlands). Horseradish peroxidase linked sheep

522   anti-mouse, donkey anti-rabbit and goat anti-rat (GE Healthcare, Chicago, USA).

523

524   **Statistical analysis**

525   Statistical analyses were performed with GraphPad Prism 6 (La Jolla, CA, USA) using

526   two-tailed t-test or one way-Anova with uncorrected Fisher's LSD. Data was tested for

527   normal distribution with a D'Agostino-Person normality test.

528

529   **Ethic statement**

530   *Y. enterocolitica* wild type strain WA-314 was a gift of Jürgen Heesemann (Max von

531   Pettenkofer Institute, Munich, Germany) and described elsewhere [40]. The source of

532   the other strains used here and the generation of *Yersinia* mutants is described in table 1

533   and in the Methods section.

534   Approval for the analysis of anonymized blood donations (WF-015/12) was obtained by

535   the Ethical Committee of the Ärztekammer Hamburg (Germany).

536   **Generation of Yersinia mutants**

537   *Y. enterocolitica* mutants WA-314ΔYopB and WA-314ΔYopD were generated as

538   described previously [42]. Briefly, mutants were constructed by replacing the coding

539   region of *yopB and yopD* by a kanamycin resistance cassette in the pYV plasmid. Correct

540   replacement of the respective *yop* genes by the resistance cassettes was verified by PCR

541   and SDS-PAGE of secreted Yop proteins and Western blotting. To rule out any unwanted

542   recombination in the chromosome due to the action of Redα and Redβ, the mutated

543   plasmids were transferred to the pYV-cured strain WA-C.

544

545   **Cell culture and transfection**

546   Hela cells (ACC#57, DSMZ-German Collection of Microorganisms and Cell Cultures) were

547   cultured at 37°C and 5% CO_2 in DMEM (Invitrogen, GIBCO, Darmstadt, Germany)

548   supplemented with 10% FCS. For infection with bacteria, HeLa cells were seeded in 6

549   well plates ($3x10^5$ cells per well) or on glass coverslips (12mm, No. 1.5H for high

23

550   resolution, Marienfeld GmbH, Lauda-Königshafen, Germany) at a density of $5x10^4$. HeLa

551   cells   were   transfected   with   turbofect   (Thermo   Fisher   Scientific,   Waltham,

552   Massachusetts, USA) for 8-16h according to the manufacturer's protocol.

553   Human peripheral blood monocytes were isolated from heparinized blood as described

554   previously [71]. Monocytes/Macrophages were cultured in RPMI1640 (Invitrogen)

555   containing 20% heterologous human serum for 7 days with medium changes every

556   three days. For immunostaining, $1x10^5$ macrophages were seeded on coverslips (12 mm,

557   No. 1.5H, Marienfeld GmbH) one day prior to infection. Macrophages were transfected

558   with the Neon Transfection System (Invitrogen) with 5 µg DNA per 10^6 cells (1000 V, 40

559   ms, 2 pulses).

560

561   **Preparation of bacteria**

562   *Yersinia* were grown in Luria Bertani (LB) broth (supplemented with suitable antibiotics

563   and diaminopimelic acid as stated in Table 1) at 27°C overnight and then diluted 1:20 in

564   fresh broth, followed by cultivation at 37°C for 1.5 h to induce expression of the T3SS.

565   Secretion of Yops was induced by calcium depletion of the *Yersinia* growth medium as

566   described before [72]. Bacteria were centrifuged and resuspended in ice-cold PBS

567   (secretion condition) or in PK solution (500 µg/ml in PBS, secretion + PK) at RT for 10

568   min, followed by incubation with 4 mM PMSF in PBS. For immunostaining, bacteria were

569   attached to gelatin (0.2 %) coated coverslips and fixed with 4% para-formaldehyde

570   (PFA; Electron Microscopy Science, Hatfield, USA) for 5 min. Biotinylation of bacteria

571   was performed with EZ-Link™ Sulfo-NHS-SS-Biotin (Thermo Fisher Scientific) as

572   described previously [64]. For cell infection, bacteria were centrifuged, resuspended in

573   ice-cold PBS and added to target cells at a multiplicity of infection (MOI) of 10-100 for 5

574   to 120 min, as indicated. Target cells in *Yersinia* containing growth medium were

24

575   centrifuged at 200 x g for 2 min to synchronize the bacterial attachment. Thereafter cells

576   were washed twice with PBS to remove unbound bacteria.

577

578   **Immunofluorescence staining**

579   Samples were fixed with 4% PFA in PBS for 5 min and permeabilized with 0.1% Triton

580   X-100 (w/v) in PBS for 10 min. Unspecific binding sites were blocked with 3% bovine

581   serum albumin (BSA, w/v) in PBS for at least 30 min. Bacterial samples were treated

582   with 0.1% Triton X-100 in PBS for non-permeabilizing conditions or with 2% SDS (w/v)

583   in PBS for permeabilizing conditions. Samples were then incubated with a 1:100 dilution

584   of the indicated primary antibody for 1 h, washed three times with PBS and incubated

585   with a 1:200 dilution of the suitable fluorophore-coupled secondary antibody for 45

586   min. Both, primary and secondary antibodies were applied in PBS supplemented with

587   3% BSA. Fluorophore-coupled phalloidin (1:200, Invitrogen) and 4',6-diamidino-2-

588   phenylindole (DAPI; 300 nM, Invitrogen) were added to the secondary antibody staining

589   solution as indicated. Colocalization studies using STED microscopy were performed

590   with Abberior-StarRed and AlexaFluor-594 labelled secondary antibodies. For staining

591   of biotinylated yersiniae Cy5-conjugated streptavidin (strep-Cy5; 1:100, Thermo Fisher

592   Scientific) was added to the primary antibody staining solution. Coverslips were

593   mounted in MOWIOL (Calbiochem, Darmstadt, Germany), ProLond Diamond (Thermo

594   Fisher Scientific) or Abberior mount liquid antifade (Abberior).

595

596   **Microscopy and high resolution imaging**

597   Fixed samples were analyzed with confocal laser scanning microscopes (Leica TCS SP5

598   or SP8) equipped with a 63x, NA1.4 oil immersion objective and Leica LAS AF or LAS X

599   SP8 software (Leica Microsystems, Wetzlar, Germany) were used for acquisition,

600   respectively. STED and corresponding confocal microscopy were carried out in

601   sequential line scanning mode using two Abberior STED setups. The first was based on

602   an Olympus IX microscope body and made use of 100x NA 1.4 oil immersion objective

603   for fluorescence excitation and detection. The second setup, used for colocalization

604   studies, was based on a Nikon Ti-E microscope body with perfect focus system and

605   employed for excitation and detection of the fluorescence signal a 60x (NA 1.4) P-Apo oil

606   immersion objective. Two pulsed lasers were used for excitation at 561 and 640 nm and

607   near-infrared pulsed laser (775 nm) for depletion. The detected fluorescence signal was

608   directed through a variable sized pinhole (set to match 1 Airy at 640 nm) and detected

609   by novel state of the art avalanche photo diodes APDs with appropriate filter settings for

610   Cy3 (605-635 nm) and Cy5 (615-755 nm). Images were recorded with a dwell time of 10

611   µs and the voxel size was set to be 20x20x150 nm for 2D-STED or 40x40x40 nm for 3D-

612   STED. The acquisitions were carried out in time gating mode i.e. with a time gating

613   width of 8ns and a delay of 781ps (Cy3) and 935ps (Cy5). 3D-STED images were

614   acquired with 80% 3D donut. 3D-STED z-stacks were background subtracted and

615   colocalization events were quantified using the ImageJ plugin JACoP. STED spots of 3D-

616   STED images were quantified with Imaris v6.1.1. (Bitplane, Zürich, CH). After baseline

617   subtraction, each channel was analyzed individually with settings adjusted to confocal

618   or STED. Background subtraction was applied in order to detect single spots. An average

619   spot was measured (diameter of largest sphere 0.3-0.45 µm for confocal and 0.11-0.24

620   µm for STED) and the Gaussian filter was adjusted to the diameter of the largest sphere.

621   Local maxima were filtered by size and quality of spots, which is defined by the intensity

622   at the center of the spot.

623

624   **Analysis of clusters formed by YopB/YopD spots visualized with STED**

625   STED spot detection and segmentation was done with Imaris (v6.1.1) on 3D-STED

626   images as described above. Segmentation analysis provided information about volume

627   and position of single STED spots which was then evaluated by a cluster analysis in

628   Matlab (S2 MatLab script, written by AF; Version 9.2, The MathWorks Inc., Natick, USA).

629   In brief, the radius of each spot was calculated through its volume and the resulting

630   sphere was placed at the position of the centre of mass of the segmented volume. The

631   spot size was defined as the full width at half maximum (FWHM) of a fluorescence

632   profile (resolution ~100 nm). Distances between the centers of mass were calculated

633   and categorized into clusters. The threshold for spots included in a cluster was defined

634   by the sum of the radiuses of two spheres. For visualization of STED clusters they were

635   projected in different colors in a superresolution 3D image.

636

637   **3D-SIM (structured illumination microscopy) superresolution microscopy**

638   We used 3D structured illumination microscopy to visualize the GFP-tagged basal body

639   component YscD together with an antibody staining against the pore proteins YopB/D.

640   Cells were imaged with a CFI Apochromat TIRF 100x Oil / NA 1.49 objective (Nikon,

641   Tokio, Japan) on a Nikon N-SIM E equipped with a Ti eclipse inverted microscope

642   (Nikon). Images were acquired using NIS Elements software steering a LU-N3-SIM

643   488/561/640 laser unit, an Orca flash 4.0 LT (Hamamatsu Photonics, Hamamatsu,

644   Japan) sCMOS or Ultra EM-CCD DU-897 (Andor Technology, Belfast, Northern Ireland)

645   camera, a Piezo z drive (Mad city labs, Wisconsin, USA), a N-SIM motorized quad band

646   filter combined with N-SIM 488 and 561 bandpass emission filters using laser lines 488

647   and 561 at 100% output power and adjustable exposure times of (300-800 msec). Z

648   stacks were acquired at 200 nm step size, covering about 1.6-2.2 μm. Reconstruction

27

649   was performed with the stack reconstruction tool (Nikon, NIS-Elements) using default

650   parameters.

651

652   **Image analysis of SIM data**

653   Particle detection was done with the ImageJ plugin TrackMate v3.5.1 [73] followed by a

654   nearest neighborhood analysis in Matlab (Version 9.2). In brief, single z-planes of 3D 2-

655   color SIM images were used for analysis. Distinct spots of GFP-YscD and YopB/D were

656   detected with Trackmate using an estimated blob diameter of 0.3 micron for both

657   channels, individually set thresholds and activated median filter. The resulting x/y

658   coordinates were exported into xml files and imported into Matlab by parseXML

659   (github.com/samuellab). The euclidean nearest neighbors of GFP-YscD spots for every

660   YopB/D spot were detected with the function Knnsearch and the resulting distances

661   were plottet. Scripts (written by JB) can be found in S2 MatLab script.

662

663   **Immunoelectron microscopy**

664   For TEM analysis, Hela cells were transfected with myc-Rac1Q61L for 16 h and infected

665   with E40 GFP-YscD at a ratio of 50:1 for 1 h. Samples were washed with ice-cold PBS and

666   then fixed with a double-strength fixative made of 4% PFA (w/v) with 0.2%

667   glutaraldehyde (GA) in PB. Fixative was replaced after 10 min with fresh single strength

668   fixative (2% PFA with 0.1% GA in PB for 20 min) at RT. Fixation was followed by three

669   wash steps with PBS at RT. Samples were then warmed up at 37°C and coated with 1%

670   gelatin. Sedentary cells were harvested carefully and spinned down in the same fixative.

671   Suspended cells were embedded in 12% (w/v) gelatin in PBS at 37°C for 5 min and the

672   pellet was solidified on ice. Small blocks were cut and infiltrated in 2.3 M sucrose

673   overnight. Thereafter the blocks were mounted on specimen holders and frozen by

674   immersing them in liquid nitrogen. Ultrathin sections (70 nm) were cut and labeled

675   according to Slot and Geuze [58]. Briefly, sections were collected on Carbon-Formvar-

676   coated nickel grids (Science Services GmbH, München, Germany). Anti-GFP-biotin

677   (1:300) was recognized with secondary anti-biotin (1:10 000) and 15 nm large protein A

678   gold; anti-YopD (1:50) with 10 nm large protein A gold in single and double labelling

679   experiments.   Sections were examined in an EM902 (Zeiss, Oberkochen, Germany).

680   Pictures were taken with a TRS 2K digital camera (A. Tröndle, Moorenweis, Germany) at

681   30.000x magnifcation.

682   Labelling intensities in randomly selected images were quantified as described

683   previously [74, 75]. Briefly, compartments of interest were defined for each antigen (Fig

684   3E; YscD: bacterial cytoplasm, bacterial double membrane and host cell; YopD: bacterial

685   cytoplasm, injectisome range, host cell). Labelling intensities were then analyzed by

686   counting colloidal gold particles per compartment. Superimposed test-point lattices

687   were used to estimate the compartment area and to count chance encounters with

688   compartments. Labelling densities (gold/µm^2), expected golds (n$_e$) and relative

689   labelling indices (RLI) with partial chi-squared values were then calculated from

690   observed and expected gold distributions to determine the preferentially labelled

691   compartments [75]. For a combined analysis of volume and surface occupying

692   compartments an acceptance zone adjacent to membranes was defined and this zone

693   was treated as a profile area [76].

694

695   **Detection of released effector and translocator proteins (Digitonin Lysis Assay)**

696   Released effector (YopH) and translocator proteins (YopB/D) were analyzed as

697   described previously [63]. In brief, HeLa cells were infected with a MOI of 100 for 1 h

698   and subsequently washed with PBS to remove non-adherent bacteria. To remove

29

699   extracellular effectors, cells were treated with PK (500 mg/ml in PBS) for 20 min at

700   room temperature. Prior to cell lysis, protease activity was blocked by the addition of

701   PMSF (4 mM in PBS). HeLa cells were lysed by the addition of digitonin (0.5% w/v in

702   PBS) at room temperature for 20 min, with repeated vortexing. Cell debris and attached

703   bacteria were separated from the lysate containing the released effectors by

704   centrifugation. The resulting supernatants and pellets were analyzed by SDS-PAGE,

705   transferred to a PVDF membrane (Immobilon-P, Millipore), and analyzed by Western

706   blot using antisera against YopH, YopB and YopD and antibodies against actin, calnexin

707   and myc-tag.

Acknowledgements

References

719

720   1. Diepold A, Kudryashev M, Delalez NJ, Berry RM, Armitage JP. Composition,

721   formation, and regulation of the cytosolic c-ring, a dynamic component of the type III

722   secretion injectisome. PLoS Biol. 2015;13:e1002039.

723   doi:10.1371/journal.pbio.1002039.

724   2. Deng W, Marshall NC, Rowland JL, McCoy JM, Worrall LJ, Santos AS, et al. Assembly,

725   structure, function and regulation of type III secretion systems. Nat Rev Microbiol.

726   2017;15:323–37. doi:10.1038/nrmicro.2017.20.

727   3. Galán JE, Lara-Tejero M, Marlovits TC, Wagner S. Bacterial type III secretion systems:

728   specialized nanomachines for protein delivery into target cells. Annu Rev Microbiol.

729   2014;68:415–38. doi:10.1146/annurev-micro-092412-155725.

730   4. Abby SS, Rocha EPC. The non-flagellar type III secretion system evolved from the

731   bacterial flagellum and diversified into host-cell adapted systems. PLoS Genet.

732   2012;8:e1002983. doi:10.1371/journal.pgen.1002983.

733   5. Pinaud L, Sansonetti PJ, Phalipon A. Host Cell Targeting by Enteropathogenic

734   Bacteria T3SS Effectors. Trends Microbiol. 2018;26:266–83.

735   doi:10.1016/j.tim.2018.01.010.

736   6. Galán JE, Waksman G. Protein-Injection Machines in Bacteria. Cell. 2018;172:1306–

737   18. doi:10.1016/j.cell.2018.01.034.

738   7. Bai F, Li Z, Umezawa A, Terada N, Jin S. Bacterial type III secretion system as a

739   protein delivery tool for a broad range of biomedical applications. Biotechnol Adv.

740   2018;36:482–93. doi:10.1016/j.biotechadv.2018.01.016.

741   8. Anantharajah A, Mingeot-Leclercq M-P, van Bambeke F. Targeting the Type Three

742   Secretion System in Pseudomonas aeruginosa. Trends Pharmacol Sci. 2016;37:734–

743   49. doi:10.1016/j.tips.2016.05.011.

744   9.   Marshall NC, Finlay BB. Targeting the type III secretion system to treat bacterial

745   infections.   Expert   Opin   Ther   Targets.   2014;18:137–52.

746   doi:10.1517/14728222.2014.855199.

747   10. Rüssmann H, Shams H, Poblete F, Fu Y, Galán JE, Donis RO. Delivery of epitopes by

748   the Salmonella type III secretion system for vaccine development. Science.

749   1998;281:565–8.

750   11. Dewoody RS, Merritt PM, Marketon MM. Regulation of the Yersinia type III secretion

751   system: traffic   control.   Front   Cell   Infect   Microbiol.   2013;3:4.

752   doi:10.3389/fcimb.2013.00004.

753   12. Portaliou AG, Tsolis KC, Loos MS, Zorzini V, Economou A. Type III Secretion: Building

754   and Operating a Remarkable Nanomachine. Trends Biochem Sci. 2016;41:175–89.

755   doi:10.1016/j.tibs.2015.09.005.

756   13. Kudryashev M, Stenta M, Schmelz S, Amstutz M, Wiesand U, Castaño-Díez D, et al. In

757   situ structural analysis of the Yersinia enterocolitica injectisome. Elife.

758   2013;2:e00792. doi:10.7554/eLife.00792.

759   14. Matteï P-J, Faudry E, Job V, Izoré T, Attree I, Dessen A. Membrane targeting and pore

760   formation by the type III secretion system translocon. FEBS J. 2011;278:414–26.

761   doi:10.1111/j.1742-4658.2010.07974.x.

762   15. Cornelis GR. The type III secretion injectisome. Nat Rev Microbiol. 2006;4:811–25.

763   doi:10.1038/nrmicro1526.

764   16. Akopyan K, Edgren T, Wang-Edgren H, Rosqvist R, Fahlgren A, Wolf-Watz H, Fallman

765   M. Translocation of surface-localized effectors in type III secretion. Proc Natl Acad

766   Sci U S A. 2011;108:1639–44. doi:10.1073/pnas.1013888108.

767   17. Mueller CA, Broz P, Cornelis GR. The type III secretion system tip complex and

768   translocon.   Mol   Microbiol.   2008;68:1085–95.   doi:10.1111/j.1365-

769   2958.2008.06237.x.

770   18. Håkansson S, Schesser K, Persson C, Galyov EE, Rosqvist R, Homblé F, Wolf-Watz H.

771   The YopB protein of Yersinia pseudotuberculosis is essential for the translocation of

772   Yop effector proteins across the target cell plasma membrane and displays a

773   contact-dependent membrane disrupting activity. EMBO J. 1996;15:5812–23.

774   19. Holmström A, Petterson J, Rosqvist R, Håkansson S, Tafazoli F, Fällman M, et al. YopK

775   of Yersinia pseudotuberculosis controls translocation of Yop effectors across the

776   eukaryotic cell membrane. Mol Microbiol. 1997;24:73–91.

777   20. Blocker A, Gounon P, Larquet E, Niebuhr K, Cabiaux V, Parsot C, Sansonetti P. The

778   tripartite type III secreton of Shigella flexneri inserts IpaB and IpaC into host

779   membranes. J Cell Biol. 1999;147:683–93.

780   21. Neyt C, Cornelis GR. Insertion of a Yop translocation pore into the macrophage

781   plasma membrane by Yersinia enterocolitica: requirement for translocators YopB

782   and YopD, but not LcrG. Mol Microbiol. 1999;33:971–81.

783   22. Dacheux D, Goure J, Chabert J, Usson Y, Attree I. Pore-forming activity of type III

784   system-secreted proteins leads to oncosis of Pseudomonas aeruginosa-infected

785   macrophages. Mol Microbiol. 2001;40:76–85.

786   23. Miki T, Okada N, Shimada Y, Danbara H. Characterization of Salmonella

787   pathogenicity island 1 type III secretion-dependent hemolytic activity in Salmonella

788   enterica   serovar   Typhimurium.   Microb   Pathog.   2004;37:65–72.

789   doi:10.1016/j.micpath.2004.04.006.

790   24. Ide T, Laarmann S, Greune L, Schillers H, Oberleithner H, Schmidt MA.

791   Characterization of translocation pores inserted into plasma membranes by type III-

792   secreted Esp proteins of enteropathogenic Escherichia coli. Cell Microbiol.

793   2001;3:669–79.

794   25. Romano FB, Tang Y, Rossi KC, Monopoli KR, Ross JL, Heuck AP. Type 3 Secretion

795   Translocators Spontaneously Assemble a Hexadecameric Transmembrane Complex.

796   J Biol Chem. 2016;291:6304–15. doi:10.1074/jbc.M115.681031.

797   26. Montagner C, Arquint C, Cornelis GR. Translocators YopB and YopD from Yersinia

798   enterocolitica form a multimeric integral membrane complex in eukaryotic cell

799   membranes. J Bacteriol. 2011;193:6923–8. doi:10.1128/JB.05555-11.

800   27. Aepfelbacher M, Roppenser B, Hentschke M, Ruckdeschel K. Activity modulation of

801   the bacterial Rho GAP YopE: an inspiration for the investigation of mammalian Rho

802   GAPs. Eur J Cell Biol. 2011;90:951–4. doi:10.1016/j.ejcb.2010.12.004.

803   28. Sheahan K-L, Isberg RR. Identification of mammalian proteins that collaborate with

804   type III secretion system function: involvement of a chemokine receptor in

805   supporting translocon activity. MBio. 2015;6:e02023-14. doi:10.1128/mBio.02023-

806   14.

807   29. Misselwitz B, Dilling S, Vonaesch P, Sacher R, Snijder B, Schlumberger M, et al. RNAi

808   screen of Salmonella invasion shows role of COPI in membrane targeting of

809   cholesterol and Cdc42. Mol Syst Biol. 2011;7:474. doi:10.1038/msb.2011.7.

810   30. Nichols CD, Casanova JE. Salmonella-directed recruitment of new membrane to

811   invasion foci via the host exocyst complex. Curr Biol. 2010;20:1316–20.

812   doi:10.1016/j.cub.2010.05.065.

813   31. Viboud GI, Bliska JB. A bacterial type III secretion system inhibits actin

814   polymerization to prevent pore formation in host cell membranes. EMBO J.

815   2001;20:5373–82. doi:10.1093/emboj/20.19.5373.

816   32. Mejía E, Bliska JB, Viboud GI. Yersinia controls type III effector delivery into host

817   cells   by   modulating   Rho   activity.   PLoS   Pathog.   2008;4:e3.

818   doi:10.1371/journal.ppat.0040003.

819   33. Köberle M, Klein-Günther A, Schütz M, Fritz M, Berchtold S, Tolosa E, et al. Yersinia

820   enterocolitica targets cells of the innate and adaptive immune system by injection of

821   Yops   in   a   mouse   infection   model.   PLoS   Pathog.   2009;5:e1000551.

822   doi:10.1371/journal.ppat.1000551.

823   34. Schweer J, Kulkarni D, Kochut A, Pezoldt J, Pisano F, Pils MC, et al. The cytotoxic

824   necrotizing factor of Yersinia pseudotuberculosis (CNFY) enhances inflammation

825   and Yop delivery during infection by activation of Rho GTPases. PLoS Pathog.

826   2013;9:e1003746. doi:10.1371/journal.ppat.1003746.

827   35. Wolters M, Boyle EC, Lardong K, Trülzsch K, Steffen A, Rottner K, et al. Cytotoxic

828   necrotizing factor-Y boosts Yersinia effector translocation by activating Rac protein.

829   J Biol Chem. 2013;288:23543–53. doi:10.1074/jbc.M112.448662.

830   36. Brubaker, R. R., Surgalla, M. J. The effect of Ca++ and Mg++ on lysis, growth, and

831   production of virulence antigens by pasteurella pestis. J Infect Dis. 1964;114:13–25.

832   37. Michiels T, Wattiau P, Brasseur R, Ruysschaert JM, Cornelis G. Secretion of Yop

833   proteins by Yersiniae. Infect Immun. 1990;58:2840–9.

834   38. Straley SC, Plano GV, Skrzypek E, Haddix PL, Fields KA. Regulation by Ca2+ in the

835   Yersinia low-Ca2+ response. Mol Microbiol. 1993;8:1005–10.

836   39. Hell SW, Wichmann J. Breaking the diffraction resolution limit by stimulated

837   emission: stimulated-emission-depletion fluorescence microscopy. Opt Lett.

838   1994;19:780–2.

839   40. Heesemann J, Laufs R. Construction of a mobilizable Yersinia enterocolitica virulence

840   plasmid. J Bacteriol. 1983;155:761–7.

841   41. Oellerich MF, Jacobi CA, Freund S, Niedung K, Bach A, Heesemann J, Trülzsch K.

842   Yersinia enterocolitica infection of mice reveals clonal invasion and abscess

843   formation. Infect Immun. 2007;75:3802–11. doi:10.1128/IAI.00419-07.

844   42. Trülzsch K, Sporleder T, Igwe EI, Rüssmann H, Heesemann J. Contribution of the

845   major secreted yops of Yersinia enterocolitica O:8 to pathogenicity in the mouse

846   infection model. Infect Immun. 2004;72:5227–34. doi:10.1128/IAI.72.9.5227-

847   5234.2004.

848   43. Marketon MM, DePaolo RW, DeBord KL, Jabri B, Schneewind O. Plague bacteria

849   target   immune   cells   during   infection.   Science.   2005;309:1739–41.

850   doi:10.1126/science.1114580.

851   44. Durand EA, Maldonado-Arocho FJ, Castillo C, Walsh RL, Mecsas J. The presence of

852   professional phagocytes dictates the number of host cells targeted for Yop

853   translocation   during   infection.   Cell   Microbiol.   2010;12:1064–82.

854   doi:10.1111/j.1462-5822.2010.01451.x.

855   45. Pettersson J, Holmström A, Hill J, Leary S, Frithz-Lindsten E, Euler-Matell A von, et al.

856   The V-antigen of Yersinia is surface exposed before target cell contact and involved

857   in virulence protein translocation. Mol Microbiol. 1999;32:961–76.

858   46. Broz P, Mueller CA, Müller SA, Philippsen A, Sorg I, Engel A, Cornelis GR. Function

859   and molecular architecture of the Yersinia injectisome tip complex. Mol Microbiol.

860   2007;65:1311–20. doi:10.1111/j.1365-2958.2007.05871.x.

861   47. Derewenda U, Mateja A, Devedjiev Y, Routzahn KM, Evdokimov AG, Derewenda ZS,

862   Waugh DS. The structure of Yersinia pestis V-antigen, an essential virulence factor

863   and   mediator   of   immunity   against   plague.   Structure.   2004;12:301–6.

864   doi:10.1016/j.str.2004.01.010.

865 48. Deane JE, Roversi P, Cordes FS, Johnson S, Kenjale R, Daniell S, et al. Molecular model

866   of a type III secretion system needle: Implications for host-cell sensing. Proc Natl

867   Acad Sci U S A. 2006;103:12529–33. doi:10.1073/pnas.0602689103.

868 49. Johnson S, Roversi P, Espina M, Olive A, Deane JE, Birket S, et al. Self-chaperoning of

869   the type III secretion system needle tip proteins IpaD and BipD. J Biol Chem.

870   2007;282:4035–44. doi:10.1074/jbc.M607945200.

871 50. Zhang Y, Lara-Tejero M, Bewersdorf J, Galán JE. Visualization and characterization of

872   individual type III protein secretion machines in live bacteria. Proc Natl Acad Sci U S

873   A. 2017;114:6098–103. doi:10.1073/pnas.1705823114.

874 51. Hu B, Lara-Tejero M, Kong Q, Galán JE, Liu J. In Situ Molecular Architecture of the

875   Salmonella Type III Secretion Machine. Cell. 2017;168:1065-1074.e10.

876   doi:10.1016/j.cell.2017.02.022.

877 52. Mueller CA, Broz P, Müller SA, Ringler P, Erne-Brand F, Sorg I, et al. The V-antigen of

878   Yersinia forms a distinct structure at the tip of injectisome needles. Science.

879   2005;310:674–6. doi:10.1126/science.1118476.

880 53. Journet L, Agrain C, Broz P, Cornelis GR. The needle length of bacterial injectisomes

881   is determined by a molecular ruler. Science. 2003;302:1757–60.

882   doi:10.1126/science.1091422.

883 54. Gustafsson MGL, Shao L, Carlton PM, Wang CJR, Golubovskaya IN, Cande WZ, et al.

884   Three-dimensional resolution doubling in wide-field fluorescence microscopy by

885   structured illumination. Biophys J. 2008;94:4957–70.

886   doi:10.1529/biophysj.107.120345.

887 55. Schermelleh L, Carlton PM, Haase S, Shao L, Winoto L, Kner P, et al. Subdiffraction

888   multicolor imaging of the nuclear periphery with 3D structured illumination

889   microscopy. Science. 2008;320:1332–6. doi:10.1126/science.1156947.

890   56. Griffiths G. Fine Structure Immunocytochemistry. Berlin, Heidelberg: Springer Berlin

891   Heidelberg; 1993.

892   57. Koster AJ, Klumperman J. Electron microscopy in cell biology: integrating structure

893   and function. Nat Rev Mol Cell Biol. 2003;Suppl:SS6-10.

894   58. Slot JW, Geuze HJ. Cryosectioning and immunolabeling. Nat Protoc. 2007;2:2480–91.

895   doi:10.1038/nprot.2007.365.

896   59. Aili M, Isaksson EL, Carlsson SE, Wolf-Watz H, Rosqvist R, Francis MS. Regulation of

897   Yersinia Yop-effector delivery by translocated YopE. Int J Med Microbiol.

898   2008;298:183–92. doi:10.1016/j.ijmm.2007.04.007.

899   60. Aepfelbacher M, Wolters M. Acting on Actin: Rac and Rho Played by Yersinia. Curr

900   Top Microbiol Immunol. 2017;399:201–20. doi:10.1007/82_2016_33.

901   61. Black DS, Bliska JB. The RhoGAP activity of the Yersinia pseudotuberculosis

902   cytotoxin YopE is required for antiphagocytic function and virulence. Mol Microbiol.

903   2000;37:515–27.

904   62. Pawel-Rammingen U von, Telepnev MV, Schmidt G, Aktories K, Wolf-Watz H,

905   Rosqvist R. GAP activity of the Yersinia YopE cytotoxin specifically targets the Rho

906   pathway: a mechanism for disruption of actin microfilament structure. Mol

907   Microbiol. 2000;36:737–48.

908   63. Nordfelth R, Wolf-Watz H. YopB of Yersinia enterocolitica is essential for YopE

909   translocation.   Infect   Immun.   2001;69:3516–8.   doi:10.1128/IAI.69.5.3516-

910   3518.2001.

911   64. Sarantis H, Balkin DM, Camilli P de, Isberg RR, Brumell JH, Grinstein S. Yersinia entry

912   into host cells requires Rab5-dependent dephosphorylation of PI(4,5)P$_2$ and

913   membrane   scission.   Cell   Host   Microbe.   2012;11:117–28.

914   doi:10.1016/j.chom.2012.01.010.

915   65. Bahnan W, Boettner DR, Westermark L, Fällman M, Schesser K. Pathogenic Yersinia

916   Promotes Its Survival by Creating an Acidic Fluid-Accessible Compartment on the

917   Macrophage   Surface.   PLoS   ONE.   2015;10:e0133298.

918   doi:10.1371/journal.pone.0133298.

919   66. Wong K-W, Mohammadi S, Isberg RR. The polybasic region of Rac1 modulates

920   bacterial uptake independently of self-association and membrane targeting. J Biol

921   Chem. 2008;283:35954–65. doi:10.1074/jbc.M804717200.

922   67. Alrutz MA, Srivastava A, Wong KW, D'Souza-Schorey C, Tang M, Ch'Ng LE, et al.

923   Efficient uptake of Yersinia pseudotuberculosis via integrin receptors involves a

924   Rac1-Arp   2/3   pathway   that   bypasses   N-WASP   function.   Mol   Microbiol.

925   2001;42:689–703.

926   68. Wong K-W, Isberg RR. Arf6 and phosphoinositol-4-phosphate-5-kinase activities

927   permit bypass of the Rac1 requirement for beta1 integrin-mediated bacterial uptake.

928   J Exp Med. 2003;198:603–14. doi:10.1084/jem.20021363.

929   69. Liu J, Park D, Lara-Tejero M, Galan JE, Li W, Waxham MN, Hu B. Visualization of the

930   type III secretion mediated Salmonella -host cell interface using cryo-electron

931   tomography; 2018.

932   70. Schmid A, Neumayer W, Trülzsch K, Israel L, Imhof A, Roessle M, et al. Cross-talk

933   between type three secretion system and metabolism in Yersinia. J Biol Chem.

934   2009;284:12165–77. doi:10.1074/jbc.M900773200.

935   71. Linder S, Nelson D, Weiss M, Aepfelbacher M. Wiskott-Aldrich syndrome protein

936   regulates podosomes in primary human macrophages. Proc Natl Acad Sci U S A.

937   1999;96:9648–53.

938   72. Heesemann J, Gross U, Schmidt N, Laufs R. Immunochemical analysis of plasmid-

939   encoded proteins released by enteropathogenic Yersinia sp. grown in calcium-

940   deficient media. Infect Immun. 1986;54:561–7.

941   73. Tinevez J-Y, Perry N, Schindelin J, Hoopes GM, Reynolds GD, Laplantine E, et al.

942   TrackMate: An open and extensible platform for single-particle tracking. Methods.

943   2017;115:80–90. doi:10.1016/j.ymeth.2016.09.016.

944   74. Griffiths G, Hoppeler H. Quantitation in immunocytochemistry: correlation of

945   immunogold labeling to absolute number of membrane antigens. J Histochem

946   Cytochem. 1986;34:1389–98. doi:10.1177/34.11.3534077.

947   75. Mayhew TM, Lucocq JM, Griffiths G. Relative labelling index: a novel stereological

948   approach to test for non-random immunogold labelling of organelles and

949   membranes on transmission electron microscopy thin sections. J Microsc.

950   2002;205:153–64.

951   76. Mayhew TM, Lucocq JM. Quantifying immunogold labelling patterns of cellular

952   compartments when they comprise mixtures of membranes (surface-occupying)

953   and organelles (volume-occupying). Histochem Cell Biol. 2008;129:367–78.

954   doi:10.1007/s00418-007-0375-6.

955

956 **Figure captions**

957 **Figure 1. Translocators YopB and YopD decorate the *Yersinia* cell surface after**

958 **secretion by the T3SS. (A) Analysis of YopB- and YopD expression.** Lysates of

959 *Yersinia* WA-314 (wild type) grown at 27°C, 37°C (high Ca^{2+}/non-secretion) or 37°C

960 (low Ca^{2+}/secretion) were subjected to SDS-PAGE and analyzed by Western blot for

961 expression of YopB, YopD or PepC, as loading control. **(B) and (C)**

962 **Immunofluorescence staining of YopB in bacterial cells under secretion and non-**

963 **secretion and cell permeabilizing and non-permeabilizing conditions**. Confocal

964 immunofluorescence and corresponding differential interference contrast (DIC) images

965 of *Yersinia* WA-314 subjected to indicated conditions. Diagrams depict fluorescence

966 intensity profiles (arbitray units, a.u.) along the arrows in the images. Scale bars: 1 μm.

967 **(C)** Quantitative analysis of YopB positive bacteria treated as in (B). Bars represent

968 mean ± S.D. of n=260-800 bacteria from 2-3 independent experiments. **(D) Confocal**

969 **and STED imaging of YopB and YopD.** Representative confocal and STED images (2D-

970 or 3D-STED as indicated) of surface localized YopB and YopD in wild type *Yersinia* at

971 secretion condition. Merge of YopB (green) and YopD (red) staining and

972 superimposition of YopB and YopD fluorescence intensity profiles along the arrow on

973 the bacterial surface. Scale bars: 1 μm.

974

975 **Figure 2. STED imaging of YopB and YopD during *Yersinia* infection of host cells.**

976 **(A) YopB concentrates in distinct patches on host cell associated bacteria**. HeLa

977 cells (left panel) were infected with WA-314 at a MOI of 100 for 2 h. Primary human

978 macrophages (right panel) were infected with biotinylated WA-314 at a MOI of 10 for 20

979 min. Cells were immunostained for YopB and either DAPI (left panel) or streptavidin-

980 Cy5 (strep-Cy5; right panel) stained. White outlines indicate position of the nucleus (N)

42

981 and dashed lines indicate host or bacterial cell circumference. Boxed regions in

982 overviews are depicted as 2.5-fold (left) or 5-fold (right) enlargements. Scale bars: 5 μm

983 (overviews) and 1 μm (enlargements). **(B) The fraction of YopB positive, cell-**

984 **associated bacteria is dependent on the target cell type.** HeLa cells or primary

985 human macrophages were infected with WA-314 at a MOI of 50 or 10, respectively, for

986 the indicated time points and stained as in (A). Data represent mean ± S.D. of n=4210

987 bacteria associated with HeLa cells from 2 experiments or n=3047 bacteria associated

988 with macrophages from 3 different donors **(C) YopB patches by confocal microscopy**

989 **can be resolved into distinct spots by STED microscopy.** HeLa cells were infected

990 with WA-314ΔYopE at a MOI of 100 and stained for YopB using AbberiorStarRed

991 secondary antibody. Single z-planes of parallel confocal (upper panel) and 2D-STED

992 (lower panel) recordings of two cell-associated bacteria are depicted in overviews.

993 Dashed lines indicate bacterial circumference. Scale bar: 1 μm. Boxed region in

994 overviews are depicted as 10-fold enlargements on the right. Scale bar: 0.1 μm. The

995 number of distinct YopB signals per bacterium (WA-314YopΔE) was quantified by

996 parallel recordings of z-stacks in confocal and 3D-STED mode. Bars represent mean ±

997 S.D. of n=27 YopB positive bacteria from two independent experiments; *p < 0.0001 **(C')**

998 **YopB spots are organised in clusters on the bacterial surface.** Myc-Rac1Q61L

999 transfected HeLa cells were infected with WA-314 at a MOI of 50 for 1 h and stained

1000 with anti-YopB antibody and Abberior635P secondary antibody. Z-stacks were recorded

1001 in 3D-STED mode and YopB spots on individual bacteria were subjected to image

1002 analysis (Methods). Identified clusters (consisting of at least 2 YopB spots) are projected

1003 in different colors and angles in a superresolution 3D image of a representative

1004 bacterium. Xyz-coordinate axes and arrows indicate position and horizontal or vertical

1005 rotation of the bacterium (see also S1 movie) Scale bar: 1 μm **(D) YopB/YopD and**

1006 **YopB/LcrV colocalize in STED images.** WA-314ΔYopE infected HeLa cells were

1007 coimmunostained for YopB (secondary antibody AlexaFluor-594) and either YopD

1008 (Abberior-StarRed) or LcrV (Abberior-StarRed). All images show representative single

1009 planes of z-stacks recorded in 3D-STED mode. Insets represent an xz projection at the

1010 level of the dashed line. Representation of colocalizing points was generated using the

1011 "Colocalization" plugin in ImageJ. Scale bar: 1 μm **(D')** Merge (yellow) of green (YopD)

1012 and red (YopB) fluorescence. Superimposed intensity profiles of YopB and YopD

1013 fluorescence along the arrow in merge.

1014

1015 **Figure 3. Spatial coupling of translocators YopB/YopD to basal body component**

1016 **YscD. (A) Schematic representation of the *Yersinia* type 3 secretion injectisome.**

1017 Positions of YopB/YopD, LcrV, YscF and GFP-YscD and the approximate length of basal

1018 body, needle, tip complex and translocon of a virtual injectisome are indicated [13, 52,

1019 53, 69]. Host membrane (HM), outer membrane (OM), inner membrane (IM). **(B) SIM**

1020 **separates YopB dots from near neighboring patches of GFP-YscD.** HeLa cells were

1021 infected with *Y. enterocolitica* E40 GFP-YscD, stained with anti-YopB antibody and z-

1022 stacks of YopB positive bacteria were recorded with SIM. A 3D reconstruction of a

1023 representative bacterium is depicted (see also S2 movie). Scale bar: 1 μm. Fluorescence

1024 intensity profiles along the longitudinal axis (arrow) of a GFP-YscD/YopB pair indicate a

1025 distance of 90 nm between fluorescence maxima. **(C) Nearest neighbor distance**

1026 **analysis of YopB/D and GFP-YscD fluorescence signals.** HeLa cells were infected with

1027 *Y. enterocolitica* E40 GFP-YscD, stained with anti-YopD or anti-YopB antibody and z-

1028 stacks of YopB/D positive bacteria were recorded with SIM. Coordinates of clearly

1029 discernible individual YopB or YopD and GFP-YscD signals were retrieved from single z-

1030 planes using ImageJ plugin TrackMate. Distances of individual YopB or YopD dots to the

1031   nearest GFP-YscD patches were analyzed by a nearest neighborhood analysis in Matlab

1032   and are depicted as histogram (mean ± S.D. was 109 ± 4 nm; 424 pairs measured;

1033   Methods). Corresponding YopB/YscD pairs (red and green) complying with a distance

1034   limit of 200 nm were plotted back on the original fluorescence images (white dots in

1035   GFP-YscD and YopB images) for illustration. Scale bar: 1 μm. **(D)** Double

1036   immunostaining of YscF and YopB in E40 GFP-YscD infected HeLa cells followed by SIM

1037   reveals conjugated fluorescence triplets displaying basal body (green), needle (white)

1038   and translocon (red). Dashed line indicates bacterial circumference. Scale bars: 100 nm.

1039   **(E) Enrichment of YopD within the injectisome range**. Transmission electron

1040   microscopy (TEM) images were compartmentalized into bacterial cytoplasm (yellow),

1041   bacterial double membrane (red), injectisome range (green, 90 nm from bacterial outer

1042   membrane) and adjacent host cell (grey). Scale bar: 100 nm. Relative labelling indices of

1043   YopD were determined for the injectisome range and the adjacent HeLa cell (n=80 golds

1044   evaluated). Relative labelling indices of GFP-YscD were calculated for bacterial

1045   cytoplasm, bacterial double membrane and the host cell (n=580 golds evaluated). *p <

1046   0.00001 different from expected distribution (S1 Tables A-C, analysis according to [75])

1047   **(E') Double immunogold staining of YopD and GFP-YscD.** HeLa cells expressing myc-

1048   Rac1Q61L were infected with *Y. enterocolitica* E40 GFP-YscD and subjected to ultrathin

1049   sectioning and immunogold staining of GFP-YscD (15 nm particles) and YopD (10 nm

1050   particles). TEM images show exemplary membrane engulfed bacteria with a GFP-

1051   YscD/YopD configuration (≤ 140 nm apart; Methods) indicative of a translocon

1052   containing/fully assembled injectisome. Scale bars: 100 nm.

1053

1054   **Figure 4. Rac1 activity and host cell type regulate translocon formation. (A) Lack**

1055   **of Rac1 inhibitor YopE and Rac1Q61L overexpression enhance translocon**

1056 **formation**. Native HeLa cells were infected with WA-314 or WA-314ΔYopE and myc-

1057 Rac1Q61L overexpressing HeLa cells were infected with WA-314 at a MOI of 50 for 1 h.

1058 Cells were immunostained for YopB and myc as well as DAPI stained. Dashed lines

1059 indicate host cell circumference. Scale bars: 5 μm. The percentage of YopB positive

1060 bacteria of total cell associated DAPI-stained bacteria was determined. Bars represent

1061 mean ± S.D. of YopB positive bacteria per cell-associated bacteria. In total n=6505 WA-

1062 314 and n=5640 WA-314ΔYopE bacteria were investigated in 4 independent

1063 experiments (upper graph); n=3423 bacteria (WA-314) associated to control

1064 transfected cells and n=7882 bacteria (WA-314) on myc-Rac1Q61L transfected cells

1065 were investigated in 3 independent experiments (lower graph). **(B) Digitonin**

1066 **extraction reveals increased incorporation of YopB and YopD into host cell**

1067 **membranes upon Rac1Q61L overexpression or lack of Rac1 inhibitor YopE**.

1068 Experimental conditions as in (A) but with a MOI of 100. HeLa cells were lyzed with

1069 digitonin and resulting supernatants (containing membrane integrated and soluble Yops

1070 from host cells) and cell pellets (containing intact bacteria and digitonin insoluble cell

1071 components) were analyzed with Western blot for the indicated proteins. YopH serves

1072 as marker for effector translocation, myc indicates myc-Rac1QL61 expression, calnexin

1073 serves as host cell loading control and HSP60 serves as bacterial loading and lysis

1074 control. Data are representative of 3 independent experiments. **(C) Quantification of**

1075 **YopB spots per bacterium using STED microscopy**. Experimental conditions for Hela

1076 cell infection as in (A). Human primary macrophages (Mφ) were infected with WA-314

1077 or WA-314ΔYopE at a MOI of 20 for 20 min. Cells were immunostained with anti-YopB

1078 antibody followed by AbberiorStarRed or Abberior635P secondary antibody. Z-stacks of

1079 YopB positive bacteria were recorded in 3D-STED mode. The number of YopB spots per

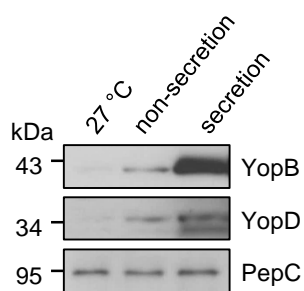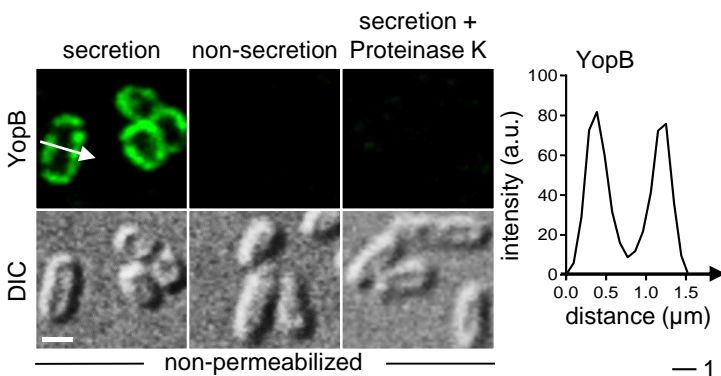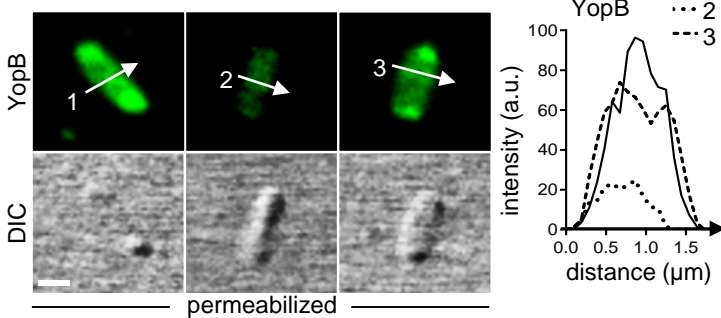1080 bacterium was analyzed using Imaris software (Methods). Bars represent mean ± S.D. of
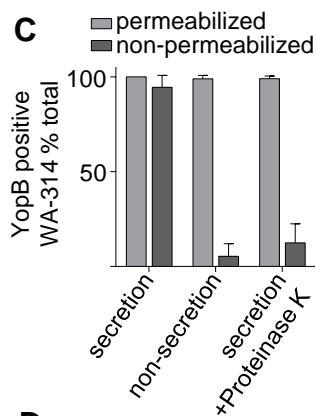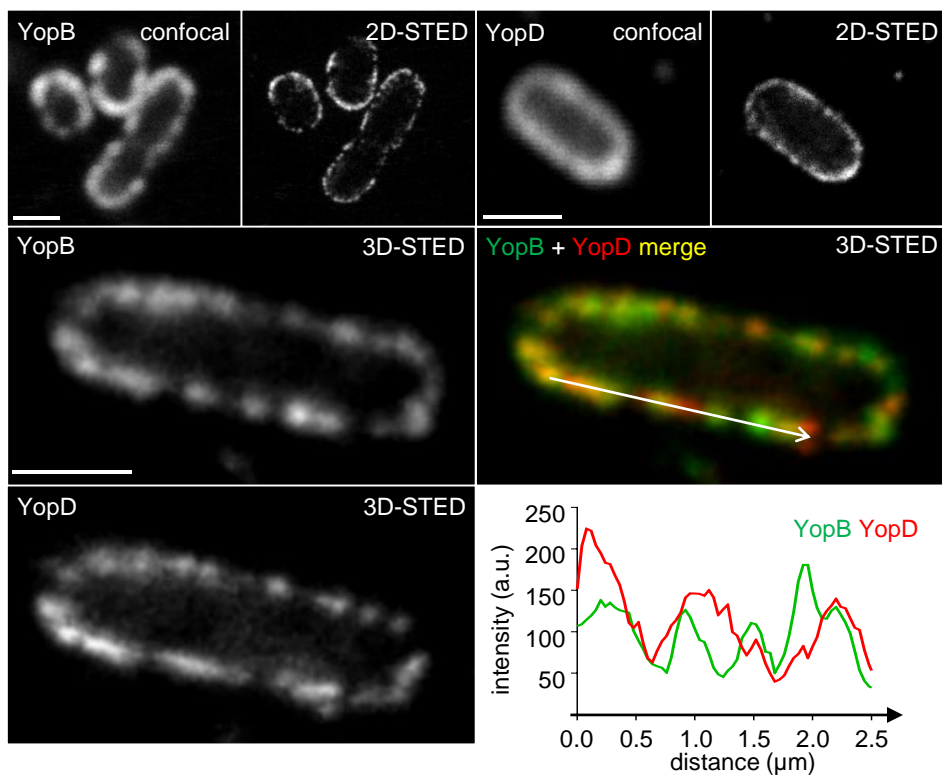
46

1081   n=20 WA-314 (Hela), n=27 WA-314ΔYopE (Hela), n=77 WA-314 (Mφ) and n=7 WA-

1082   314ΔYopE (Mφ) bacteria investigated in 2-3 independent experiments. *p < 0.05, **p <

1083   0.01 **(D) YopB positive WA-314 and WA-314ΔYopE in macrophages at different**

1084   **infection times.** Primary human macrophages were infected with WA-314 or WA-

1085   314ΔYopE at a MOI of 10 for the indicated time periods. The percentage of YopB positive

1086   bacteria of total cell associated bacteria was calculated. Data represent mean ± S.D. of

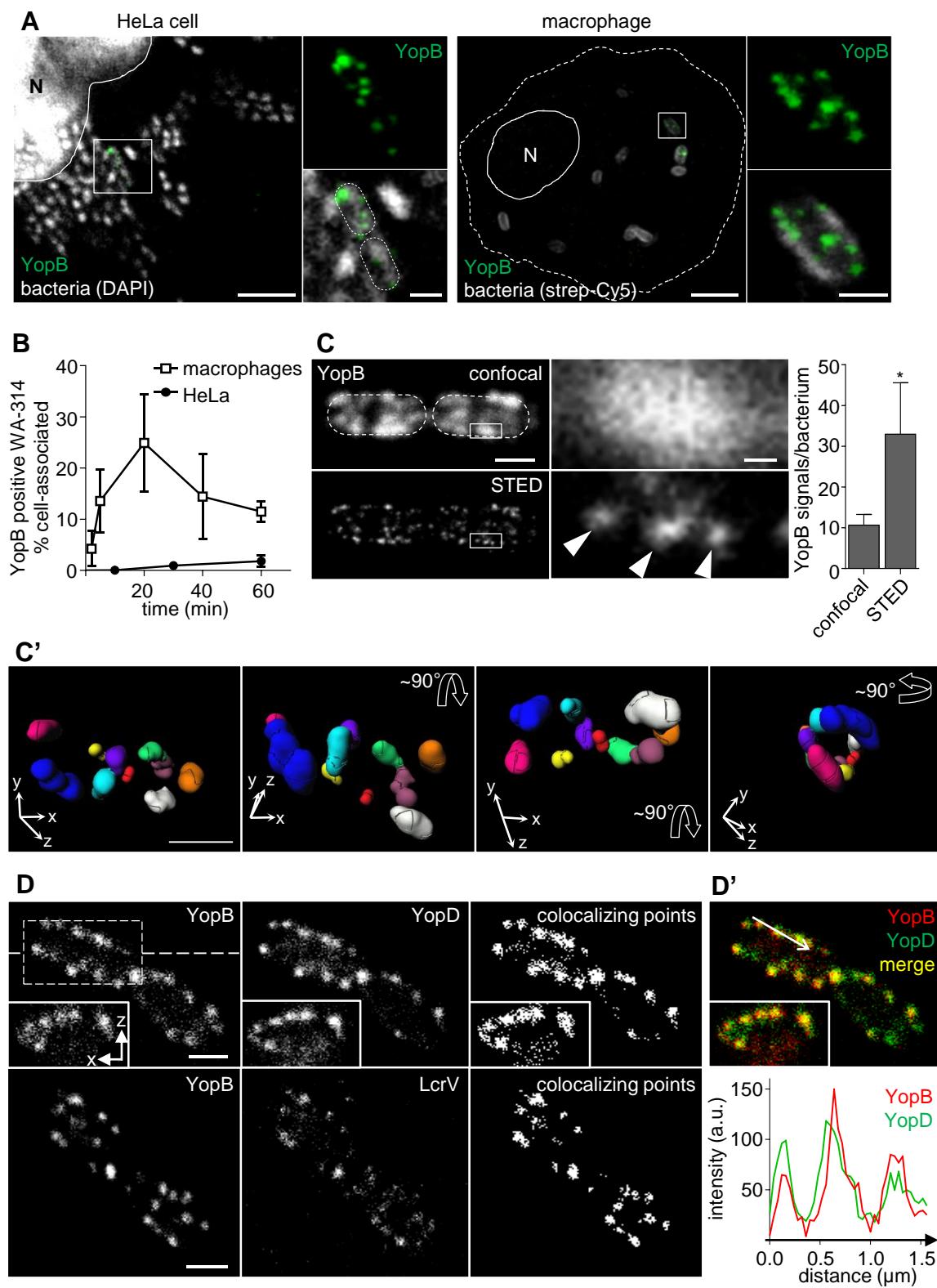1087   n=3047 WA-314 and n=1822 WA-314ΔYopE in 2-3 independent experiments.

1088

1089   **Figure 5. Formation of translocons is triggered in a prevacuole, a PI(4,5)P2**

1090   **enriched intermediary host cell compartment. (A-A'') YopB positive bacteria**

1091   **reside in an intermediary compartment.** Hela cells were infected with surface-

1092   biotinylated WA-314 at a MOI of 20 for 60 min and were immunostained using anti-LPS

1093   antibody and stained with streptavidin-Cy5 without cell permeabilization. Then cells

1094   were permeabilized and immunostained with anti-YopB antibody. **(A)** Images of a

1095   bacterial chain showing YopB staining only in the part of the chain located in the

1096   intermediary compartment (red in merge) but not in the outside location (yellow in

1097   merge). **(A')** Image of a YopB positive bacterium (white) in the inside compartment (no

1098   red or green). Scale bar: 1 μm **(A'')** Distribution of YopB positive bacteria between

1099   intermediary, inside and outside compartments. Bars represent mean ± S.D. of n=95

1100   YopB positive bacteria recorded in 2 independent experiments. **(B) Bacterial passage**

1101   **from the outside into the intermediary and inside compartments of macrophages.**

1102   Primary human macrophages of donors 1-4 were infected with biotinylated WA-314 at a

1103   MOI of 10 for the indicated time points and stained with anti-LPS antibody, streptavidin-

1104   Cy5 and DAPI to score their localization to the indicated compartments as in (A-A'').

1105   Data represent mean of at least n=1000 bacteria investigated per donor. **(C) YopB**
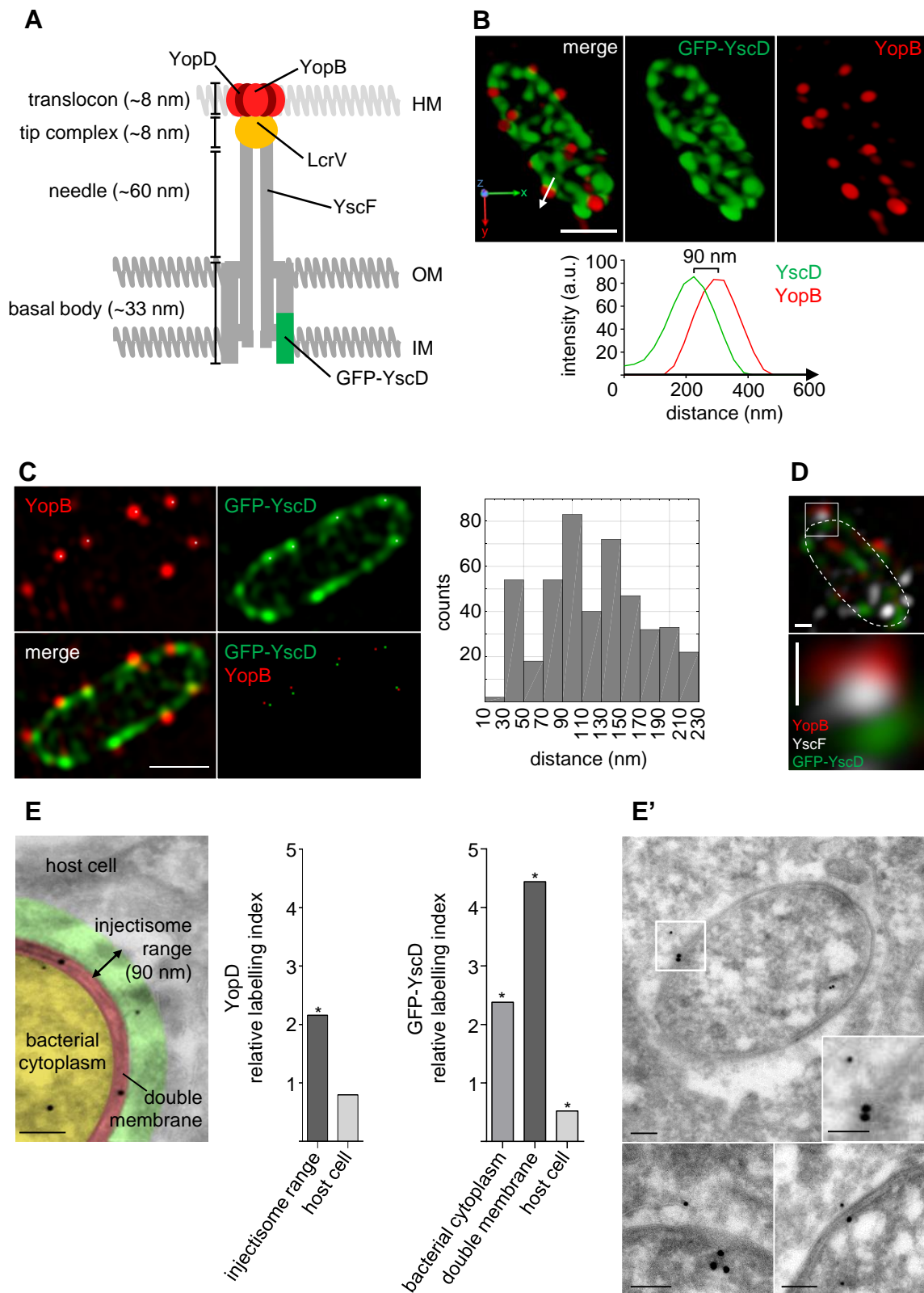
1106 **positive bacteria passage from the intermediary to the inside compartment in**

1107 **macrophages.** Experimental conditions as in (B) but with no LPS but YopB

1108 immunostaining. Data represent mean of n=952 YopB positive bacteria investigated in 1

1109 donor. **(D) Intermediary compartment is marked by PLCδ-PH-GFP.** Hela cells

1110 expressing PLCδ-PH-GFP and myc-Rac1Q61L were infected with WA-314 at a MOI of 10

1111 for 60 min, stained with anti-LPS antibody and streptavidin-Cy5. Bacteria with PLCδ-PH-

1112 GFP enrichment were judged for their localization as in (A-A''). Bars represent mean ±

1113 S.D. of n=398 PLCδ-PH-GFP positive bacteria investigated in 1 experiment. **(E) PLCδ-PH-**

1114 **GFP enrichment around YopB positive bacteria in human macrophages.** Primary

1115 human macrophages expressing PLCδ-PH-GFP were infected with WA-314 at a MOI of

1116 20 for 20 min and immunostained for YopB. **(F) External addition of proteinase K to**

1117 **infected HeLa cells degrades YopB and YopD but not YopH.** Control or myc-

1118 Rac1Q61L expressing HeLa cells were infected with WA-314 or WA-314ΔYopE at a MOI

1119 of 100 for 1 h as indicated. Cells were incubated with PK for 20 min. PK was inactivated

1120 with PMSF, cells were extracted with digitonin and analyzed by Western blot for YopB

1121 and YopD, YopH (translocated effector protein), myc (myc-Rac1Q61L expression) and

1122 actin (loading control). Data are representative of 3 independent experiments. **(G)**

1123 **Rac1Q61L overexpression increases uptake of WA-314 into HeLa cells.** Control or

1124 myc-Rac1Q61L expressing HeLa cells were infected with WA-314 at a MOI of 20 for 1 h,

1125 fixed and stained with anti-LPS antibody (antibody accessible bacteria in outside

1126 location) and then permeabilized and stained with the same anti-LPS antibody in

1127 combination with a different secondary antibody (antibody inaccessible bacteria in

1128 intermediary and inside compartments). Bars represent mean ± S.D. of n=1609 bacteria

1129 on control transfected cells and n=3482 bacteria on myc-Rac1Q61L transfected cells

1130 investigated in 3 independent experiments. **(H) Rac1L61 expression significantly**

1131   **increases the number of YopB positive bacteria in the intermediary and inside**

1132   **compartments.** HeLa cells expressing PLCδ-PH-GFP and either empty vector (control)

1133   or myc-Rac1Q61L were infected with WA-314 at a MOI of 50 for 1 h and stained with

1134   anti-YopB antibody. The number of YopB positive bacteria as fraction of total cell

1135   associated bacteria and their distribution between the intermediary (PLCδ-PH-GFP

1136   positive) and inside (PLCδ-PH-GFP negative) compartments was determined. Bars

1137   represent mean ± S.D. of n=1820 bacteria on control transfected cells and n=6020

1138   bacteria on myc-Rac1Q61L transfected cells investigated in 3 independent experiments.

Fig 1

A

B

C

D

Fig 2

A HeLa cell — macrophage

B

C

C'

D

D'

Fig 3

A

YopD
YopB
translocon (~8 nm)
HM
tip complex (~8 nm)
LcrV
needle (~60 nm)
YscF
OM
basal body (~33 nm)
IM
GFP-YscD

B

merge
GFP-YscD
YopB

90 nm
YscD
YopB
intensity (a.u.)
distance (nm)

C

YopB
GFP-YscD
merge
GFP-YscD
YopB

counts
distance (nm)

D

YopB
YscF
GFP-YscD

E

host cell
injectisome range (90 nm)
bacterial cytoplasm
double membrane

YopD relative labelling index
injectisome range
host cell

GFP-YscD relative labelling index
bacterial cytoplasm
double membrane
host cell

E'

Fig 4

Fig 5

A

α-LPS YopB | strep-Cy5 YopB | merge α-LPS strep-Cy5 YopB

A' merge α-LPS strep-Cy5 YopB

yellow=outside; red=intermediary; arrowhead: inside

A''

YopB positive WA-314 %

intermediary, inside, outside

B

● outside ■ intermediary ▲ inside

cell-associated WA-314 %

donor 1, donor 2, donor 3, donor 4

time (min)

C

■ intermediary ▲ inside

YopB positive WA-314 %

time (min)

D

α-LPS strep-Cy5 PLCδ1-PH merge

PLCδ1-PH positive WA-314 %

intermediary, inside

E

PLCδ1-PH YopB | PLCδ1-PH | YopB

F

	WA-314		WA-314 ΔYopE		WA-314		
myc-Rac1Q61L	-	-	-	-	+	+	kDa
PK	-	+	-	+	-	+	
YopH							55
YopB							40
YopD							35
actin							40
myc							25

G

antibody inaccessible WA-314 %

control, myc-Rac1Q61L

H

YopB positive WA-314 % cell-associated

▭ intermediary/PLCδ1-PH ▨ inside

control, myc-Rac1Q61L